



Research article

Insights into dengue transmission modeling: Index of memory, carriers, and vaccination dynamics explored via non-integer derivative

Rashid Jan¹, Imtiaz Ahmad², Hijaz Ahmad^{3,4,5}, Narcisa Vranceanu^{6,*} and Adrian Gheorghe Hasegan⁷

- ¹ Institute of Energy Infrastructure (IEI), Department of Civil Engineering, College of Engineering, Universiti Tenaga Nasional (UNITEN), Putrajaya Campus, Jalan IKRAM-UNITEN, 43000 Kajang, Selangor, Malaysia
- ² Institute of Informatics and Computing in Energy (IICE), Universiti Tenaga Nasional, Kajang, Selangor, Malaysia
- ³ Department of Mathematics, Faculty of Science, Islamic University of Madinah, Madinah, Saudi Arabia
- ⁴ Near East University, Operational Research Center in Healthcare, TRNC Mersin 10, Nicosia, 99138, Turkey
- ⁵ Department of Mathematics and Informatics, Azerbaijan University, Jeyhun Hajibeyli street, 71, AZ1007, Baku, Azerbaijan
- ⁶ Faculty of Engineering, Department of Industrial Machines and Equipments, “Lucian Blaga” University of Sibiu, Romania, 10 Victoriei Boulevard
- ⁷ Lucian Blaga University of Sibiu, Faculty of Medicine, 2A Lucian Blaga Str., 550169, Sibiu, Romania

* **Correspondence:** Email: vranceanu.narcisai@ulbsibiu.ro.

Abstract: It is acknowledged that dengue infection has a significant economic impact due to healthcare costs and lost productivity. Research can provide insights into the economic burden of the disease, guiding policymakers in their allocation of resources for prevention and control interventions. In this work, we structured a novel mathematical model that describes the spread of dengue with the effects of carriers, an index of memory and vaccination. To show the effect of treatment on the dynamics of dengue, we have incorporated medication-related treatment into the system. The proposed dynamics are represented by using fractional derivatives to capture the role of memory in the control of the infection. We introduced the fundamental principles and notions of non-integer derivatives for the analysis of the model; moreover, the existence and uniqueness results for the solution of the system have been established with the help of mathematical skills. The theory of fixed points has been utilized for the analysis and examination of the system. We have established

Ulam-Hyers stability for the recommended system of dengue infection. Regarding the numerical findings, a numerical method is presented to highlight the solution pathways for the system of dengue infection. Several simulations have been performed to visualize the contribution of the input parameters of the system to the prevention and control of the infection. The index of memory, vaccination, and treatment are suggested to be attractive parameters which can reduce the level of infection while the biting rate, asymptomatic carriers and transmission rate are critical as they can increase the risk of the infection in society. Our findings not only provide information for the effective management of the infection they also possess valuable insights that can improve public health.

Keywords: dengue infection; epidemic models; fractional calculus; asymptomatic carriers; numerical solution; dynamical behavior

1. Introduction

Dengue fever, a renowned tropical disease provoked by dengue viruses and predominantly spread by female *Aedes aegypti* mosquitoes, has become a global health concern, affecting public health and economies in approximately 128 countries worldwide due to the impact of global warming [1]. Currently, dengue fever is widespread in the majority of sub-tropical and tropical regions across the world. The spread of this disease has notably intensified within urban and semi-urban areas in recent periods. Approximately 2.5 billion individuals globally are exposed to the potential threat posed by dengue fever [2, 3]. Upon being bitten by an infective mosquito, an individual undergoes an incubation period lasting around 4 to 7 days. Following this, the individual transitions into the acute infection phase, which can range from 2 to 10 days. If female *Aedes aegypti* mosquitoes bite the individual during this initial stage of illness, they might contract the virus, thus initiating a potential new cycle of transmission. The infection presents a range of signs and symptoms, including headache, vomiting, high fever, nausea, red eyes, bone pain, aches, severe weakness, muscle pain, lower back pain, joint pain, rash, pain behind the eyes, and severe fatigue. Transmission of the virus occurs when a mosquito becomes infected after feeding on the blood of an infected individual and subsequently spreads the virus to others. Infected mosquitoes remain carriers throughout their entire lifespan, with limited instances of vertical transmission of the dengue virus reported [4, 5]. The increasing prevalence of dengue infections in recent decades has driven significant efforts toward the development of dengue vaccines. While some countries have access to dengue infection vaccines [6], fully effective vaccines have not yet been established. Researchers have introduced various control strategies to prevent dengue fever, but further research is required to identify reliable and effective strategies.

Mathematical models play a vital role in comprehending the transmission dynamics of infectious diseases, aiding in the development of effective control interventions [7–10]. Through mathematical analysis, researchers can identify key aspects of disease transmission and introduce novel control interventions. Notably, Lourdes Esteva provided a fundamental modeling concept for dengue fever, incorporating a variable human population and investigating system stability [11]. Additionally, other studies [12] focused on structuring the transmission process for dengue and examining the equilibrium stability in their proposed systems. Addressing the complexities of dengue infection, the

researchers in [13, 14] conceptualized the impact of vaccination and antibody-dependent enhancement on disease transmission. In another article [15], the authors focused on utilizing mathematical modeling while into account the complexities of serotype-specific clinical impacts and patient infection history, highlighting the significance of accurate predictions for public health planning and control strategies. In another article [16] the authors applied mathematical models to understand how vaccination impacts the transmission dynamics of dengue in Johor, Malaysia. The study focused on analyzing the effectiveness of vaccination strategies in controlling dengue spread, contributing insight that will be valuable for public health interventions in the region, whereas the authors of [17] have presented a mathematical model that explores the dynamics of dengue fever, considering both scenarios with and without awareness in the host population. The model was constructed to understand how awareness about the disease influences its spread. The study's findings provide insights into the potential impact of awareness campaigns on controlling dengue fever transmission. Furthermore, considering the significant concern posed by frequent asymptomatic cases of dengue [18], particularly in non-endemic regions, efforts have been made to incorporate them into the models. The occurrence of reinfection with dengue also presents challenges for disease control. In [19], the authors explored the unique challenges of dengue fever in the elderly, focusing on atypical presentations and heightened risks of severe dengue and hospital-acquired infections, as well as providing valuable insights for effective management in this demographic. The objective of this research was to construct a holistic model that elucidates the transmission dynamics of dengue infection, incorporating the impact of vaccination, treatment, index of memory, and the presence of asymptomatic carriers.

Fractional calculus is vital in efforts to address real-world problems [20–24] because it provides a more versatile and nuanced mathematical framework [25–29]. In various research disciplines and engineering applications, many phenomena exhibit non-integer order behaviors that cannot be accurately described by traditional calculus [30–33]. This mathematical approach finds successful application across various scientific fields, providing robust models to represent a broad spectrum of practical challenges in areas such as economics, physics, mathematics, control systems, and biology [34–36]. In the theory of fractional calculus, the two-scale methodology provides a sound explanation [37]. This innovative idea, recently developed, centers on the critical consideration of scale when analyzing practical problems [38]. It has been reported that memory significantly influences the transmission dynamics of mosquito-borne infections, particularly in the area of retaining information about their preceding stages [39, 40]. The application of fractional operators enhances the accuracy and precision of models of these phenomena. In this study, our choice was to express the dynamics of dengue infection within a fractional framework, aiming to illustrate the influence of memory on the propagation and management of dengue infection. We establish a qualitative framework that is embedded in fractional calculus to investigate the dynamics of dengue transmission. Our focus extends to exploring aspects such as vaccination, memory effects, treatment and the presence of asymptomatic carriers.

The summary of the article is given as follows:

- Section 2: Presents the essential concepts and outcomes of fractional calculus.
- Section 3: Formulates an epidemic model for the study of dengue transmission, considering vaccination, index of memory, asymptotic fraction, and treatment to enhance realism.
- Section 4: It is dedicated to the investigation of the proposed model.

- Section 5: Establishes necessary conditions for Ulam-Hyers stability.
- Section 6: Introduces a numerical approach to solving the model and examines dengue dynamics with various input factors.
- Section 7: Provides the article's conclusion and closing remarks.

2. Foundations of fractional calculus

This section outlines the essential terms and foundational principles of fractional theory that are to be applied in the analysis of the proposed model. The significant advantage of fractional calculus stems from its incorporation of the memory index, a pivotal factor shaping the transmission dynamics of dengue infection. The researchers specifically focused on fractional systems due to their broad applicability across various domains [30, 41]. Some of the basic definitions are given as follows:

Definition 2.1. ([42]). Assume that $f : \mathbb{R}^+ \rightarrow \mathbb{R}$ is a function whose fractional integral is of order $\xi > 0$, as follows:

$$\mathcal{I}_{0^+}^\xi f(s) = \frac{1}{\Gamma(\xi)} \int_0^s (s-q)^{\xi-1} f(q) dq, \quad \xi > 0, \quad (2.1)$$

the function specified on the right side of the equation is defined for the real numbers in a pointwise manner, denoted by \mathbb{R}^+ . In this article, the symbol $\Gamma(\cdot)$ represents the gamma function.

Definition 2.2. ([42]). The expression denoting the Caputo fractional derivative of the order $\xi \in (m-1, m)$ applied to a continuous function f can be stated as follows

$${}^C D_{0^+}^\xi f(s) = \mathcal{I}_{0^+}^{m-\xi} D^m f(s), \quad D = \frac{d}{dq}, \quad (2.2)$$

Specifically, for values where $0 < \xi < 1$, we obtain the following result

$${}^C D_{0^+}^\xi f(s) = \frac{1}{\Gamma(1-\xi)} \int_0^s \frac{f'(q)}{(s-q)^\xi} dq, \quad m-1 < m, \quad m \in \mathbb{N}. \quad (2.3)$$

The above equation provides the function f which is differentiable in $[0, +\infty)$, with Γ representing the function.

Theorem 2.1. ([42]). If $Re(\xi) > 0$ and m equals $[Re(\xi)] + 1$, then

$$(\mathcal{I}_{0^+}^\xi {}^C D_{0^+}^\xi f)(s) = f(s) - \sum_{i=1}^m \frac{(D_{0^+}^i f)(0^+)}{i!} s^i. \quad (2.4)$$

3. Mathematical framework for model formulation

In this conceptual framework, we establish the interrelationships between female vectors, denoted as N_h , and hosts, denoted as N_v , thereby elucidating the mechanism underlying the transmission dynamics of dengue fever. The host population is divided into distinct classes: \mathcal{S}_h for susceptible, \mathcal{V}_h for vaccinated, \mathcal{I}_{Ah} for asymptomatic infections, \mathcal{I}_h for infected individuals, and \mathcal{R}_h for those who have recovered. Meanwhile, the female mosquito population represented as N_v is categorized into

susceptible \mathcal{S}_v and infectious \mathcal{I}_v compartments. We presume that the natural birth and death rates, denoted by μ_h for the host population and μ_v for the vector population, are constant throughout both populations. In this model, the incidence rates originating from the susceptible classes (\mathcal{S}_h and \mathcal{V}_h) are given by $(\frac{b\beta_1}{N_h}\mathcal{I}_v)$ and $(\frac{b\beta_2}{N_h}\mathcal{V}_h)$, respectively. Additionally, the incidence rate from susceptible mosquitoes (\mathcal{S}_v) to infectious mosquitoes (\mathcal{I}_v) is represented by $(\frac{b\beta_3}{N_h}(\mathcal{I}_h + \mathcal{I}_{Ah}))$, where b denotes the mosquito biting rate. The asymptomatic fraction is symbolized by ψ , and the vaccination rate is given by p . In addition to this, the rate of recovery is indicated by γ_h whereas the recovery through treatment is denoted by η . Then, the dynamics of dengue can be described by the following system of equations

$$\begin{cases} \frac{d\mathcal{S}_h}{dt} = \mu_h N_h - \frac{\beta_1 b \mathcal{S}_h \mathcal{I}_v}{N_h} - p \mathcal{S}_h - \mu_h \mathcal{S}_h, \\ \frac{d\mathcal{V}_h}{dt} = p \mathcal{S}_h - \frac{\beta_2 b \mathcal{V}_h \mathcal{I}_v}{N_h} - \mu_h \mathcal{V}_h, \\ \frac{d\mathcal{I}_{Ah}}{dt} = \psi \frac{\beta_1 b \mathcal{S}_h \mathcal{I}_v}{N_h} + \psi \frac{\beta_2 b \mathcal{V}_h \mathcal{I}_v}{N_h} - (\mu_h + \gamma_h) \mathcal{I}_{Ah}, \\ \frac{d\mathcal{I}_h}{dt} = (1 - \psi) \frac{\beta_1 b \mathcal{S}_h \mathcal{I}_v}{N_h} + (1 - \psi) \frac{\beta_2 b \mathcal{V}_h \mathcal{I}_v}{N_h} - (\mu_h + \eta + \gamma_h) \mathcal{I}_h, \\ \frac{d\mathcal{R}_h}{dt} = \gamma_h \mathcal{I}_{Ah} + \gamma_h \mathcal{I}_h + \eta \mathcal{I}_h - \mu_h \mathcal{R}_h, \\ \frac{d\mathcal{S}_v}{dt} = \mu_v N_v - \frac{\beta_3 b \mathcal{S}_v (\mathcal{I}_h + \mathcal{I}_{Ah})}{N_h} - \mu_v \mathcal{S}_v, \\ \frac{d\mathcal{I}_v}{dt} = \frac{\beta_3 b \mathcal{S}_v (\mathcal{I}_h + \mathcal{I}_{Ah})}{N_h} - \mu_v \mathcal{I}_v, \end{cases} \quad (3.1)$$

with the following initial conditions

$$\mathcal{S}_h(0) \geq 0, \mathcal{V}_h(0) \geq 0, \mathcal{I}_{Ah}(0) \geq 0, \mathcal{I}_h(0) \geq 0, \mathcal{R}_h(0) \geq 0, \mathcal{S}_v(0) \geq 0, \mathcal{I}_v(0) \geq 0,$$

where β_1, β_2 and β_3 denote the transmission probabilities with the condition that $\beta_1 \geq \beta_2$. Furthermore, we have

$$N_h = \mathcal{S}_h + \mathcal{V}_h + \mathcal{I}_{Ah} + \mathcal{I}_h + \mathcal{R}_h, \quad (3.2)$$

and

$$N_v = \mathcal{S}_v + \mathcal{I}_v. \quad (3.3)$$

It is well-known that fractional calculus theory is rich in applications and produces more accurate results for the dynamics of biological phenomena. The two-scale fractal theory for population dynamics is a relatively new area of research that aims to understand the dynamics of population growth in closed systems [43]. The two-scale fractal theory for population dynamics is based on the idea that populations exhibit fractal patterns at different scales. The theory considers the effects of nonlinear diffusion and fractional spatial diffusion on population growth. In this work, we structure the dynamics of dengue in a fractional framework to obtain an understanding of the importance of memory in the spread and control of the infection. Also, the transmission dynamics of dengue involve an associative learning mechanism, where knowledge of previous stages is retained. Host population memory, connected to individual awareness, reduces contact rates between vectors and hosts. Meanwhile, mosquitoes draw from past experiences on human location, blood preference, color, and defensive behaviors to choose suitable hosts. Integrating fractional-order systems into mathematical models of dengue infection effectively captures and represents these intricate phenomena. Thus, we represent our model (3.1) of dengue infection through the use of fractional derivatives with the effect

of memory as follows:

$$\left\{ \begin{array}{l} {}^C D_{0^+}^\xi S_h(t) = \mu_h N_h - \frac{\beta_1 b S_h I_v}{N_h} - p S_h - \mu_h S_h, \\ {}^C D_{0^+}^\xi V_h(t) = p S_h - \frac{\beta_2 b V_h I_v}{N_h} - \mu_h V_h, \\ {}^C D_{0^+}^\xi I_{Ah}(t) = \psi \frac{\beta_1 b S_h I_v}{N_h} + \psi \frac{\beta_2 b V_h I_v}{N_h} - (\mu_h + \gamma_h) I_{Ah}, \\ {}^C D_{0^+}^\xi I_h(t) = (1 - \psi) \frac{\beta_1 b S_h I_v}{N_h} + (1 - \psi) \frac{\beta_2 b V_h I_v}{N_h} - (\mu_h + \eta + \gamma_h) I_h, \\ {}^C D_{0^+}^\xi R_h(t) = \gamma_h I_{Ah} + \gamma_h I_h + \eta I_h - \mu_h R_h, \\ {}^C D_{0^+}^\xi S_v(t) = \mu_v N_v - \frac{\beta_3 b S_v (I_h + I_{Ah})}{N_h} - \mu_v S_v, \\ {}^C D_{0^+}^\xi I_v(t) = \frac{\beta_3 b S_v (I_h + I_{Ah})}{N_h} - \mu_v I_v, \end{array} \right. \quad (3.4)$$

where ${}^C D_{0^+}^\xi$ indicates the Caputo fractional derivative with order ξ . Here, we focused on a time-fractional epidemic model which plays an important role in advancing our understanding of infectious diseases, providing a more realistic framework for analysis and offering valuable insights into disease dynamics. The spatial diffusion of biological populations is also an important research area in ecology and population biology. The research on the spatial diffusion of biological populations has focused on developing models that take into account nonlinear diffusion effects and fractional spatial diffusion. These models have important implications for obtaining an understanding of the dynamics of biological populations and predicting their spatial patterns [43,44]. In our future work, we will focus on fractional space diffusion systems to investigate the dynamics of infectious diseases. The following theorem is on the non-negativity and boundedness of the solutions of our proposed system, which can be easily proved through analysis.

Theorem 3.1. The solutions of our fractional model (3.4) are non-negative and bounded for non-negative initial values of state variables.

It is well-known that equilibrium points in epidemic models are essential for comprehending the dynamics of infectious diseases, guiding the development of effective control measures, and predicting the overall trajectory of an epidemic in a population. There are two meaningful equilibrium points in an epidemic model, i.e., disease-free and endemic points. The disease-free equilibrium is crucial in the assessment of the potential success of preventive and control measures. It represents a stable state in which the infection has been eliminated, providing insights into conditions that promote disease control. It is denoted by \mathcal{E}_0 and given by

$$\mathcal{E}_0 = \left(\frac{\mu_h N_h}{p + \mu_h}, \frac{p \mu_h N_h}{\mu_h (p + \mu_h)}, 0, 0, 0, N_v, 0 \right). \quad (3.5)$$

On the other hand, the endemic equilibrium is necessary to obtain an understanding of the persistent existence of the disease in a population. Analysis of this equilibrium helps to identify factors that contribute to the sustained transmission of the infection and informs strategies for long-term management and intervention. In this work, we focused on the solution behavior and Ulam-Hyers stability of the system while other aspects of the system will be investigated in our future work.

4. Existence and uniqueness results

The existence and uniqueness of solutions govern fractional-order differential equation theory. Many researchers have recently become interested in the theory; we refer to [45, 46] and the references therein for some of the recent growth. We will utilize fixed point theorems to evaluate that whether the solution of the suggested framework is real and unique. The proposed model (3.4) can be reformulated as follows:

$$\left\{ \begin{array}{l} {}^C D_{0^+}^\xi S_h(t) = \Theta_1(t, S_h, \mathcal{V}_h, \mathcal{I}_{Ah}, \mathcal{I}_h, \mathcal{R}_h, S_v, \mathcal{I}_v), \\ {}^C D_{0^+}^\xi V_h(t) = \Theta_2(t, S_h, V_h, \mathcal{I}_{Ah}, \mathcal{I}_h, \mathcal{R}_h, S_v, \mathcal{I}_v), \\ {}^C D_{0^+}^\xi \mathcal{I}_{Ah}(t) = \Theta_3(t, S_h, \mathcal{V}_h, \mathcal{I}_{Ah}, \mathcal{I}_h, \mathcal{R}_h, S_v, \mathcal{I}_v), \\ {}^C D_{0^+}^\xi \mathcal{I}_h(t) = \Theta_4(t, S_h, \mathcal{V}_h, \mathcal{I}_{Ah}, \mathcal{I}_h, \mathcal{R}_h, S_v, \mathcal{I}_v), \\ {}^C D_{0^+}^\xi \mathcal{R}_h(t) = \Theta_5(t, S_h, \mathcal{V}_h, \mathcal{I}_{Ah}, \mathcal{I}_h, \mathcal{R}_h, S_v, \mathcal{I}_v), \\ {}^C D_{0^+}^\xi S_v(t) = \Theta_6(t, S_h, \mathcal{V}_h, \mathcal{I}_{Ah}, \mathcal{I}_h, \mathcal{R}_h, S_v, \mathcal{I}_v), \\ {}^C D_{0^+}^\xi \mathcal{I}_v(t) = \Theta_7(t, S_h, \mathcal{V}_h, \mathcal{I}_{Ah}, \mathcal{I}_h, \mathcal{R}_h, S_v, \mathcal{I}_v), \end{array} \right. \quad (4.1)$$

where

$$\left\{ \begin{array}{l} \Theta_1(t, S_h, \mathcal{V}_h, \mathcal{I}_{Ah}, \mathcal{I}_h, \mathcal{R}_h, S_v, \mathcal{I}_v) = \mu_h N_h - \frac{\beta_1 b S_h \mathcal{I}_v}{N_h} - p S_h - \mu_h S_h, \\ \Theta_2(t, S_h, \mathcal{V}_h, \mathcal{I}_{Ah}, \mathcal{I}_h, \mathcal{R}_h, S_v, \mathcal{I}_v) = p S_h - \frac{\beta_2 b \mathcal{V}_h \mathcal{I}_v}{N_h} - \mu_h \mathcal{V}_h, \\ \Theta_3(t, S_h, \mathcal{V}_h, \mathcal{I}_{Ah}, \mathcal{I}_h, \mathcal{R}_h, S_v, \mathcal{I}_v) = \psi \frac{\beta_1 b S_h \mathcal{I}_v}{N_h} + \psi \frac{\beta_2 b \mathcal{V}_h \mathcal{I}_v}{N_h} - (\mu_h + \gamma_h) \mathcal{I}_{Ah}, \\ \Theta_4(t, S_h, \mathcal{V}_h, \mathcal{I}_{Ah}, \mathcal{I}_h, \mathcal{R}_h, S_v, \mathcal{I}_v) = (1 - \psi) \frac{\beta_1 b S_h \mathcal{I}_v}{N_h} + (1 - \psi) \frac{\beta_2 b \mathcal{V}_h \mathcal{I}_v}{N_h} - (\mu_h + \eta + \gamma_h) \mathcal{I}_h, \\ \Theta_5(t, S_h, \mathcal{V}_h, \mathcal{I}_{Ah}, \mathcal{I}_h, \mathcal{R}_h, S_v, \mathcal{I}_v) = \gamma_h \mathcal{I}_{Ah} + \gamma_h \mathcal{I}_h + \eta \mathcal{I}_h - \mu_h \mathcal{R}_h, \\ \Theta_6(t, S_h, \mathcal{V}_h, \mathcal{I}_{Ah}, \mathcal{I}_h, \mathcal{R}_h, S_v, \mathcal{I}_v) = \mu_v N_v - \frac{\beta_3 b S_v (\mathcal{I}_h + \mathcal{I}_{Ah})}{N_h} - \mu_v S_v, \\ \Theta_7(t, S_h, \mathcal{V}_h, \mathcal{I}_{Ah}, \mathcal{I}_h, \mathcal{R}_h, S_v, \mathcal{I}_v) = \frac{\beta_3 b S_v (\mathcal{I}_h + \mathcal{I}_{Ah})}{N_h} - \mu_v \mathcal{I}_v, \end{array} \right. \quad (4.2)$$

Therefore, model (3.4) can be summarized follows:

$$\left\{ \begin{array}{l} {}^C D_{0^+}^\xi \Psi(t) = \kappa(t, \Psi(t)); \quad t \in \mathcal{J} = [0, a]. \quad 0 < \xi \leq 1. \\ \Psi(0) = \Psi_0 \geq 0, \end{array} \right. \quad (4.3)$$

under the following circumstances:

$$\left\{ \begin{array}{l} \Psi(t) = (S_h, \mathcal{V}_h, \mathcal{I}_{Ah}, \mathcal{I}_h, \mathcal{R}_h, S_v, \mathcal{I}_v)^T, \\ \Psi(0) = (S_h, \mathcal{V}_h, \mathcal{I}_{Ah}, \mathcal{I}_h, \mathcal{R}_h, S_v, \mathcal{I}_v)^T, \\ \kappa(t, \Psi(t)) = \left(\Theta_j(t, S_h, \mathcal{V}_h, \mathcal{I}_{Ah}, \mathcal{I}_h, \mathcal{R}_h, S_v, \mathcal{I}_v) \right)^T, \quad j = 1, \dots, 7, \end{array} \right. \quad (4.4)$$

where $(.)^T$ signifies the transposition technique. From the above mentioned Theorem 2.1, (4.3) is given by

$$\Psi(t) = \Psi_0 + \mathcal{I}_{0^+}^\xi \kappa(t, \Psi(t))$$

$$= \Psi_0 + \frac{1}{\Gamma(\xi)} \int_0^t (t-q)^{\xi-1} \kappa(q, \Psi(q)) dq. \quad (4.5)$$

Consider that $F = G([0, a]; \mathbb{R})$, denoting the Banach space that comprises continuous function mappings from $[0, a]$ to \mathbb{R} . This space is equipped with a norm given by

$$\|\Psi\| = \sup_{t \in \mathcal{J}} |\Psi(t)|, \quad (4.6)$$

where

$$|\Psi(t)| = |\mathcal{S}_h(t)| + |\mathcal{V}_h(t)| + |\mathcal{V}_{Ah}(t)| + |\mathcal{I}_h(t)| + |\mathcal{R}_h(t)| + |\mathcal{S}_v(t)| + |\mathcal{I}_v(t)|, \quad (4.7)$$

and

$$\mathcal{S}_h, \mathcal{V}_h, \mathcal{I}_{Ah}, \mathcal{I}_h, \mathcal{R}_h, \mathcal{S}_v, \mathcal{I}_v \in G([0, a]). \quad (4.8)$$

Theorem 4.1. ([47]). Consider $\mathcal{M} \neq \emptyset$ to represent a closed, bounded, convex subset of a Banach space \mathbf{B} . Assume \mathcal{P}_1 and \mathcal{P}_2 to be two operators that satisfy the following relationships

- 1) If $\Psi_1, \Psi_2 \in \mathcal{M}$, then $\mathcal{P}_1\Psi_1 + \mathcal{P}_2\Psi_2 \in \mathcal{M}$;
- 2) \mathcal{P}_1 is smooth and compact.
- 3) \mathcal{P}_2 is a mapping of contractions.

Subsequently, the existence of an element denoted as U , belonging to the set \mathcal{M} , is confirmed, satisfying that $U = \mathcal{P}_1U + \mathcal{P}_2U$.

Theorem 4.2. Assuming that the continuity of the function $\kappa : \mathcal{J} \times \mathbb{R}^7 \rightarrow \mathbb{R}$, and that it satisfies condition (A1), along with the additional assumption (A2) $|\kappa(t, \Psi)| \leq \Phi(t)$ for all $(t, \Psi) \in \mathcal{J} \times \mathbb{R}^7$, where $\Phi \in G([0, a]; \mathbb{R}_+)$, it can be inferred that the suggested model (3.4) exhibits at least one solution under the condition that $\mathcal{L}\kappa\|\Psi_1(t_0) - \Psi_2(t_0)\| < 1$.

Proof. Specifying that $\|\Phi\| = \sup_{t \in \mathcal{J}} |\Phi(t)|$ and $\varsigma \geq \|\Psi_0\| + \mathcal{U}\|\Phi\|$, we assume that $\mathbf{B}_\varsigma = \{\Psi \in \mathbb{B} : \|\Psi\| \leq \varsigma\}$. Consider the operations $\mathcal{P}_1, \mathcal{P}_2$ on \mathbf{B}_ς , which are described as follows:

$$(\mathcal{P}_1\Psi)(t) = \frac{1}{\Gamma(\xi)} \int_0^t (t-q)^{\xi-1} \kappa(q, \Psi(q)) dq, \quad t \in \mathcal{J}, \text{ and } (\mathcal{P}_2\Psi)(t) = \Psi(t_0), \quad t \in \mathcal{J}.$$

Thus, for any $\Psi_1, \Psi_2 \in \mathbf{B}_\varsigma$, we have

$$\begin{aligned} \|(\mathcal{P}_1\Psi_1)(t) + (\mathcal{P}_2\Psi_2)(t)\| &\leq \|\Psi_0\| + \frac{1}{\Gamma(\xi)} \int_0^t (t-q)^{\xi-1} \kappa(q, \Psi_1(q)) dq \\ &\leq \|\Psi_0\| + \mathcal{U}\|\Phi\| \\ &\leq \varsigma < \infty. \end{aligned} \quad (4.9)$$

Hence, $\mathcal{P}_1\Psi_1 + \mathcal{P}_2\Psi_2 \in \mathbf{B}_\varsigma$.

Our next step is to prove that the operator \mathcal{P}_2 is contracted.

Considering any $t \in \mathcal{J}$ and $\Psi_1, \Psi_2 \in \mathbf{B}_\varsigma$, then the obvious solution is given by

$$\|(\mathcal{P}_2\Psi_1)(t) - (\mathcal{P}_2\Psi_2)(t)\| \leq \|\Psi_1(t_0) - \Psi_2(t_0)\|. \quad (4.10)$$

Considering the continuity of the function κ , it can be deduced that the operator \mathcal{P}_1 also exhibits continuity. Furthermore, for every $t \in \mathcal{J}$ and $\Psi_1 \in \mathbf{B}_\varsigma$, $\|\mathcal{P}_1\Psi\| \leq \mathcal{U}\|\Phi\| < +\infty$.

This implies that \mathcal{P}_1 is evenly bounded. Lastly, we demonstrate that \mathcal{P}_1 is a compact operator. Define,

$$\sup_{(t, \Psi) \in \mathcal{J} \times \mathbf{B}_\varsigma} |\kappa(t, \Psi(t))| = \kappa^*, \quad (4.11)$$

It follows that

$$\begin{aligned}
 |(\mathcal{P}_1\Psi)(t_2) - (\mathcal{P}_1\Psi)(t_1)| &= \frac{1}{\Gamma(\xi)} \left| \int_0^{t_1} [(t_2 - q)^{\xi-1} \right. \\
 &\quad - (t_1 - q)^{\xi-1}] \kappa(q, \Psi(q)) dq \\
 &\quad \left. + \int_{t_1}^{t_2} (t_2 - q)^{\xi-1} \kappa(q, \Psi(q)) dq \right| \\
 &\leq \frac{\kappa^*}{\Gamma(\xi)} [2(t_2 - t_1)^\xi + (t_2^\xi - t_1^\xi)] \\
 &\rightarrow 0, \quad \text{as } t_2 \rightarrow t_1.
 \end{aligned} \tag{4.12}$$

\mathcal{P}_1 is therefore equicontinuous on \mathbf{B}_ζ , which makes it quite compact. The Arzela-Ascoli theorem shows that \mathcal{P}_1 is compact on \mathbf{B}_ζ . Model (3.4) has at least one solution since there are no contradictions in the hypotheses of the theorem [48].

Theorem 4.3. Assuming that the function κ belongs to the set $G([\mathcal{J}, \mathbb{R}])$, it assigns a bounded subset of $\mathcal{J} \times \mathbb{R}^7$ to sets of \mathbb{R} that are relatively compact. Additionally, let $\mathcal{L}\kappa > 0$ be a fixed constant, satisfying the condition that $(\mathcal{A}1)|\kappa(t, \Psi_1(t)) - \kappa(t, \Psi_2(t))| \leq \mathcal{L}\kappa|\Psi_1(t) - \Psi_2(t)|$ for all $t \in \mathcal{J}$ and any $\Psi_1, \Psi_2 \in G([\mathcal{J}, \mathbb{R}])$. Under these conditions, the integral equation (4.5) possesses a unique distinct solution, corresponding to the model (3.4). This existence is guaranteed to exist provided that $\mathcal{U}\mathcal{L}\kappa < 1$, where $\mathcal{U} = \frac{a^\xi}{\Gamma(\xi-1)}$.

Proof. The operator is denoted as $P : \mathcal{E} \rightarrow \mathcal{E}$ and formulated by using the following definition

$$(\mathcal{P}\Psi)(t) = \Psi_0 + \frac{1}{\Gamma(\xi)} \int_0^t (t - q)^{\xi-1} \kappa(q, \Psi(q)) dq. \tag{4.13}$$

The well-defined nature of the operator P is obvious, and the fixed point of P corresponds to the unique solution of model (3.4). To demonstrate this, consider the following approach, i.e., $\sup_{t \in \mathcal{J}} \|\kappa(t, 0)\| = M_1$ and $k \geq \|\Psi_0\| + \mathcal{U}M_1$. Consequently, it is enough to prove that $P\mathcal{H}_k \subset \mathcal{H}_k$, where the set $\mathcal{H}_k = \{\Psi \in \mathcal{E} : \|\Psi\| \leq k\}$, which possesses both closed and convex properties. For any given Ψ belonging to \mathcal{H}_k , we obtain

$$\begin{aligned}
 |(\mathcal{P}\Psi)(t)| &\leq |\Psi_0| + \frac{1}{\Gamma(\xi)} \int_0^t (t - q)^{\xi-1} |\kappa(q, \Psi(q))| dq \\
 &\leq \Psi_0 + \frac{1}{\Gamma(\xi)} \int_0^t (t - q)^{\xi-1} [|\kappa(q, \Psi(q)) - \kappa(q, 0)| + |\kappa(q, 0)|] dq \\
 &\leq \Psi_0 + \frac{(\mathcal{L}_\kappa k + M_1)}{\Gamma(\xi)} \int_0^t (t - q)^{\xi-1} dq \\
 &\leq \Psi_0 + \frac{(\mathcal{L}_\kappa k + M_1)}{\Gamma(\xi) + 1} b^\xi \\
 &\leq \Psi_0 + \mathcal{U}(\mathcal{L}_\kappa k + M_1) \\
 &\leq k.
 \end{aligned} \tag{4.14}$$

Consequently, the outcomes are derived. Moreover, considering any $\Psi_1, \Psi_2 \in \mathcal{E}$, we obtain the following

$$|(\mathcal{P}\Psi_1)(t) - (\mathcal{P}\Psi_2)(t)| \leq \frac{1}{\Gamma(\xi)} \int_0^t (t - q)^{\xi-1} |\kappa(q, \Psi_1(q)) - \kappa(q, \Psi_2(q))| dq$$

$$\begin{aligned} &\leq \frac{\mathcal{L}_\kappa}{\Gamma(\xi)} \int_0^t (t-q)^{\xi-1} |\Psi_1(q) - \Psi_2(q)| dq \\ &\leq \mathcal{U} \mathcal{L}_\kappa |\Psi_1(t) - \Psi_2(t)|. \end{aligned} \quad (4.15)$$

thus indicating that

$$\|(\mathcal{P}\Psi_1)(t) - (\mathcal{P}\Psi_2)(t)\| \leq \mathcal{U} \mathcal{L}_\kappa \|\Psi_1 - \Psi_2\|. \quad (4.16)$$

Consequently, based on the Banach contraction principle, we can conclude that the suggested model (3.4) has a unique solution.

5. Stability analysis

We present the stability analysis within the Ulam-Hyers and generalized Ulam-Hyers framework to assess the suggested model (3.4) in this section. Ulam-Hyers [49, 50] originally introduced the concept of Ulam stability. The aforementioned stability has been investigated in various research articles on classical fractional derivatives, such as in [51, 52]. To ensure the stability of the approximated solutions, we chose to employ nonlinear functional analysis to examine both the Ulam-Hyers stability and the generalized stability of the presented model (3.4). For this purpose, the following definitions are necessary. Consider the following inequality, where ε represents a positive real value

$$|{}^C D_{0+}^\xi \bar{\Psi}(t) - \kappa(t, \bar{\Psi}(t))| \leq \varepsilon, \quad t \in \mathcal{J}, \quad (5.1)$$

whereas $\varepsilon = \max(\varepsilon_{\mathcal{J}})^T$, $\mathcal{J} = 1, \dots, 7$.

Definition 5.1. If $C_\kappa > 0$, the model (3.4) exhibits Ulam-Hyers stability. For any positive value ε , and for a solution $\bar{\Psi}$ belonging to the set \mathcal{E} that fulfills condition (5.1), there exists a unique solution $\Psi \in \mathcal{E}$ to (3.4).

$$|\bar{\Psi}(t) - \Psi(t)| \leq C_\kappa \varepsilon, \quad t \in \mathcal{J}, \quad (5.2)$$

provides $C_\kappa = \max(C_{\kappa_{\mathcal{J}}})^T$.

Definition 5.2. Let $\psi_\kappa : \mathbb{R}_+ \rightarrow \mathbb{R}_+$ be a continuous function with $\psi_\kappa(0) = 0$. Problem (3.4) is considered to be generalized Ulam-Hyers stable if, for every solution $\bar{\Psi} \in \mathcal{E}$ of (5.1), then there exists a solution $\Psi \in \mathcal{E}$ of (3.4) such that

$$|\bar{\Psi}(t) - \Psi(t)| \leq \psi_\kappa \varepsilon_1, \quad t \in \mathcal{J}, \text{ where } \psi_\kappa = \max(\psi_{\kappa_{\mathcal{J}}})^T.$$

Remark 5.1. The expression $\bar{\Psi} \in \mathcal{E}$ meets the requirement of (5.1), if and only if a function $g \in \mathcal{E}$ possesses the following properties:

$$|g(t)| \leq \varepsilon, \quad g = \max(g_j)^T, \quad t \in \mathcal{J}. \quad (5.3)$$

$${}^C D_{0+}^\xi \bar{\Psi}(t) = \kappa(t, \bar{\Psi}(t)) + g(t), \quad t \in \mathcal{J}. \quad (5.4)$$

Theorem 5.1. Assuming that $\bar{\Psi}$ belongs to the set \mathcal{E} and fulfills the inequality (5.1), then $\bar{\Psi}$ effects the integral inequality defined as follows in mathematical terms

$$\left| \bar{\Psi}(t) - \bar{\Psi}_0 - \frac{1}{\Gamma(\xi)} \int_0^t (t-q)^{\xi-1} \kappa(q, \bar{\Psi}(q)) dq \right| \leq \mathcal{U} \varepsilon. \quad (5.5)$$

Proof. Utilize (2) of Remark 5.1.

${}^C\mathcal{D}_{0^+}^\xi \bar{\Psi}(t) = \kappa(t, \bar{\Psi}(t)) + g(t)$ and Theorem 2.1 gives

$$\begin{aligned} \bar{\Psi}(t) = \bar{\Psi}_0 &+ \frac{1}{\Gamma(\xi)} \int_0^t (t-q)^{\xi-1} \kappa(q, \bar{\Psi}(q)) dq \\ &+ \frac{1}{\Gamma(\xi)} \int_0^t (t-q)^{\xi-1} g(q) dq. \end{aligned} \quad (5.6)$$

Utilize (1) from Remark 5.1 and (\mathcal{A}_2) from the following equation:

$$\begin{aligned} &\left| \bar{\Psi}(t) - \bar{\Psi}_0 - \frac{1}{\Gamma(\xi)} \int_0^t (t-q)^{\xi-1} \kappa(q, \bar{\Psi}(q)) dq \right| \\ &\leq \frac{1}{\Gamma(\xi)} \int_0^t (t-q)^{\xi-1} g(q) dq \\ &\leq \mathcal{U}\varepsilon. \end{aligned} \quad (5.7)$$

Hence, this is our required solution. \square

Theorem 5.2. Consider a continuous mapping $\kappa : \mathcal{J} \times \mathbb{R}^7 \rightarrow \mathbb{R}$ across the entire space of $\Psi \in \mathcal{E}$, and assume that the hypothesis $(\mathcal{A}1)$ holds with $1 - \mathcal{U}L\kappa > 0$. Consequently, the problem (3.4) demonstrates Ulam-Hyers stability as well as generalized Ulam-Hyers stability.

Proof. Assume that $\bar{\Psi} \in \mathcal{E}$ satisfies the condition of (5.1), and that $\Psi \in \mathcal{E}$ is the only single solution to (3.4). As a result, for every $\varepsilon > 0$ and $t \in \mathcal{J}$, in accordance with Lemma 5.1, we obtain

$$\begin{aligned} |\bar{\Psi}(t) - \Psi(t)| &= \max_{(t \in \mathcal{J})} \left| \bar{\Psi}(t) - \Psi_0 - \frac{1}{\Gamma(\xi)} \int_0^t (t-q)^{\xi-1} \kappa(q, \Psi(q)) dq \right| \\ &\leq \max_{(t \in \mathcal{J})} \left| \bar{\Psi}(t) - \bar{\Psi}_0 - \frac{1}{\Gamma(\xi)} \int_0^t (t-q)^{\xi-1} \kappa(q, \bar{\Psi}(q)) dq \right| \\ &\quad + \max_{(t \in \mathcal{J})} \frac{1}{\Gamma(\xi)} \int_0^t (t-q)^{\xi-1} \left| \kappa(q, \bar{\Psi}(q)) - \kappa(q, \Psi(q)) \right| dq \\ &\leq \left| \Psi(t) - \bar{\Psi}_0 - \frac{1}{\Gamma(\xi)} \int_0^t (t-q)^{\xi-1} \kappa(q, \bar{\Psi}(q)) dq \right| \\ &\quad + \frac{L_\kappa}{\Gamma(\xi)} \int_0^t (t-q)^{\xi-1} |\bar{\Psi}(q) - \Psi(q)| dq \\ &\leq \mathcal{U}\varepsilon + \mathcal{U}L_\kappa |\bar{\Psi}(t) - \Psi(t)|. \end{aligned} \quad (5.8)$$

So,

$$\|\bar{\Psi} - \Psi\| \leq C_\kappa \varepsilon, \quad (5.9)$$

where,

$$C_{\kappa} = \frac{\mathfrak{U}}{1 - \mathfrak{U}L_{\kappa}}. \quad (5.10)$$

So, we set $\psi_{\kappa}(\varepsilon) = C_{\kappa}(\varepsilon)$ such that $\psi_{\kappa}(0) = 0$. Our analysis leads us to the perfect rephrasing that the stated problem (3.4) exhibits both Ulam-Hyers stability and generalized Ulam-Hyers stability. \square

6. Numerical findings and analysis

In our investigation, we analyzed the dynamic behavior of our system (3.4) for dengue infection through numerical analysis. Employing assumed values for the state variables and input parameters, we conducted simulations to replicate different scenarios. The core aim of these numerical simulations was to illustrate the impact of input factors on the intricate dynamics of dengue, providing valuable insights into the system's behavior under various conditions. Through this approach, we seek a comprehensive understanding of the interplay between key variables and the consequential patterns that govern the progression of dengue infection. Based on our analysis, we will propose efficient strategies for controlling dengue, aiming to decrease the prevalence of infection within society. In order to demonstrate how the infection level fluctuates with the variation of different input parameters, we depict the solution pathways of the asymptomatic hosts, infected hosts and infected vectors.

In the initial scenario illustrated in Figure 1, our focus was on showcasing the impact of varying the index of memory on the infection levels within the population. This exploration was performed to determine whether the fractional parameter could function as a viable control parameter. The findings revealed the fractional parameter's significance as an influential factor, serving as a valuable tool to modulate the extent of infection within the community. The results indicated a noteworthy trend: the infection level exhibited sensitivity to changes in the index of memory. Specifically, decreasing the memory index correlated with a reduction in the infection level. This observation underscores the potential effectiveness of interventions aimed at strategically managing the fractional parameter to curtail the spread of infection. As a result, we advocate for proactive policymaking and targeted actions to adjust the memory index, offering a promising avenue for infection control measures and public health management.

In the second case illustrated in Figure 2, we explored the role of the transmission probability on the populations of infected hosts and vectors. This investigation was undertaken to elucidate the pivotal role of the transmission probability and its impact on the dynamics of the infection. The results highlighted the critical nature of the transmission probability, showcasing its substantial influence on the risk of infection. As this parameter was adjusted, we observed corresponding shifts in the populations of both infected hosts and vectors. Higher transmission probabilities were associated with a high risk of infection, emphasizing the need for careful consideration and strategic management of this parameter in disease control efforts. In the same way, Figure 3 illustrated the importance of the mosquito biting rate. Our observations indicate that these parameters hold considerable significance, possessing the capacity to heighten the risk of infection within the community.

In Figure 4, the impact of treatment on the infected classes is illustrated. Our observations indicate that the treatment rate exerts a significant level of control over the prevalence of dengue infection within the society, demonstrating its potential in efforts to mitigate the spread of the disease. Subsequently,

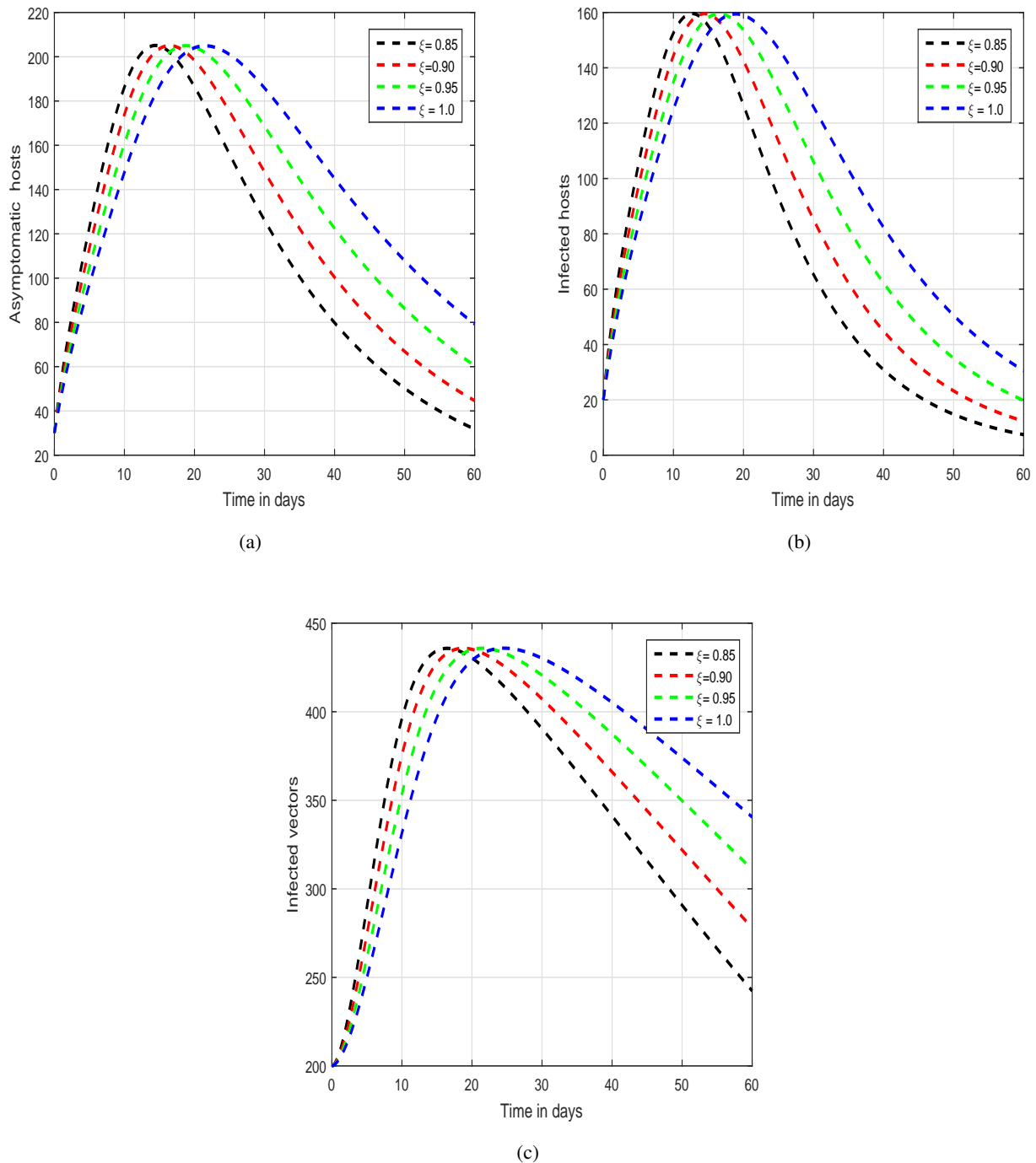


Figure 1. Visual examination was performed to analyze the dynamic characteristics of the recommended system (3.4) of dengue infection with the variation of the fractional parameter ξ , i.e., $\xi = 0.85, 0.90, 0.95$, and 1.00 .

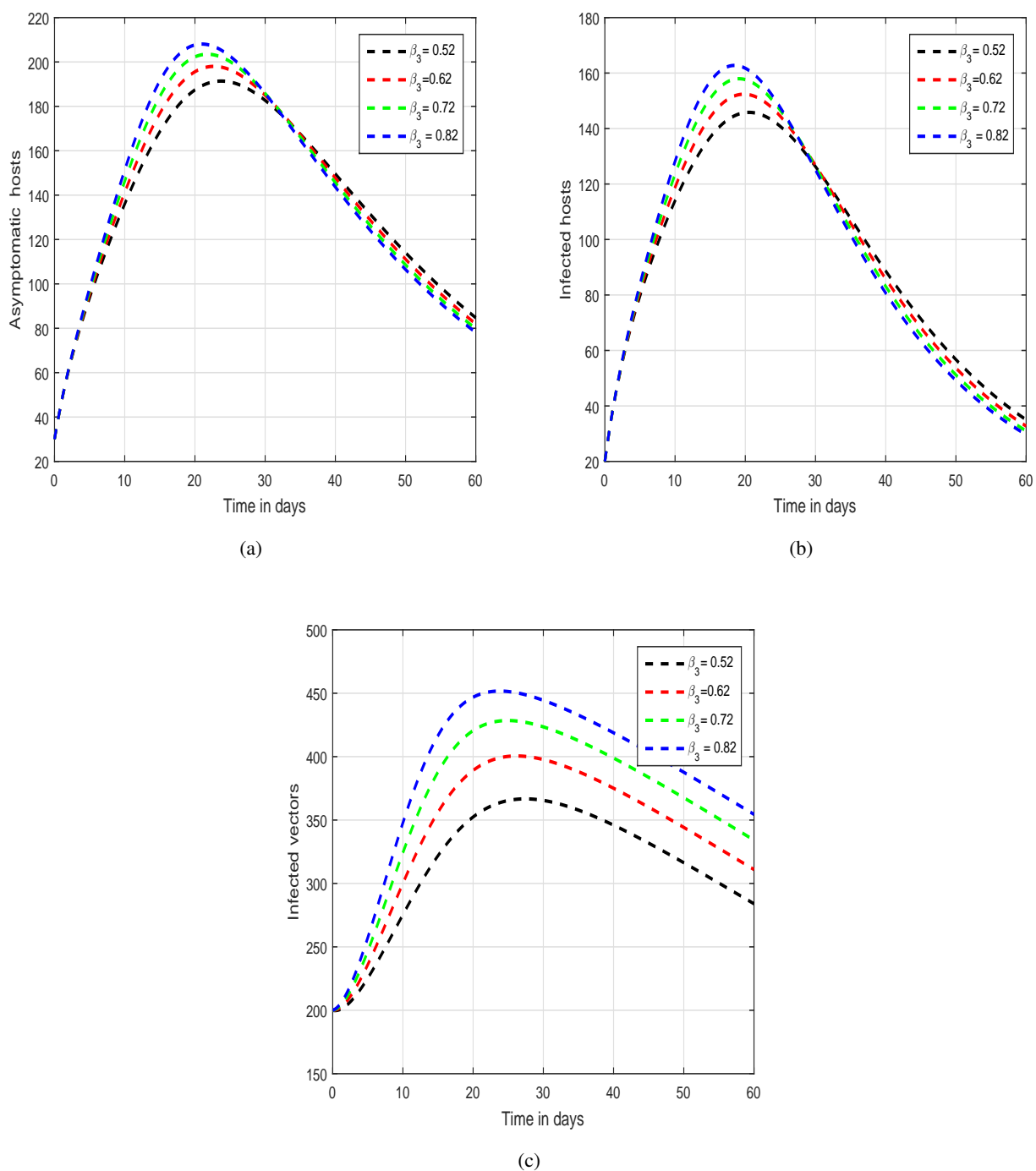


Figure 2. Depiction of the solution pathways for the recommended fractional system (3.4) of dengue infection with variation of transmission probability β_3 , i.e., $\beta_3 = 0.52, 0.62, 0.72$, and $\beta_3 = 0.82$.

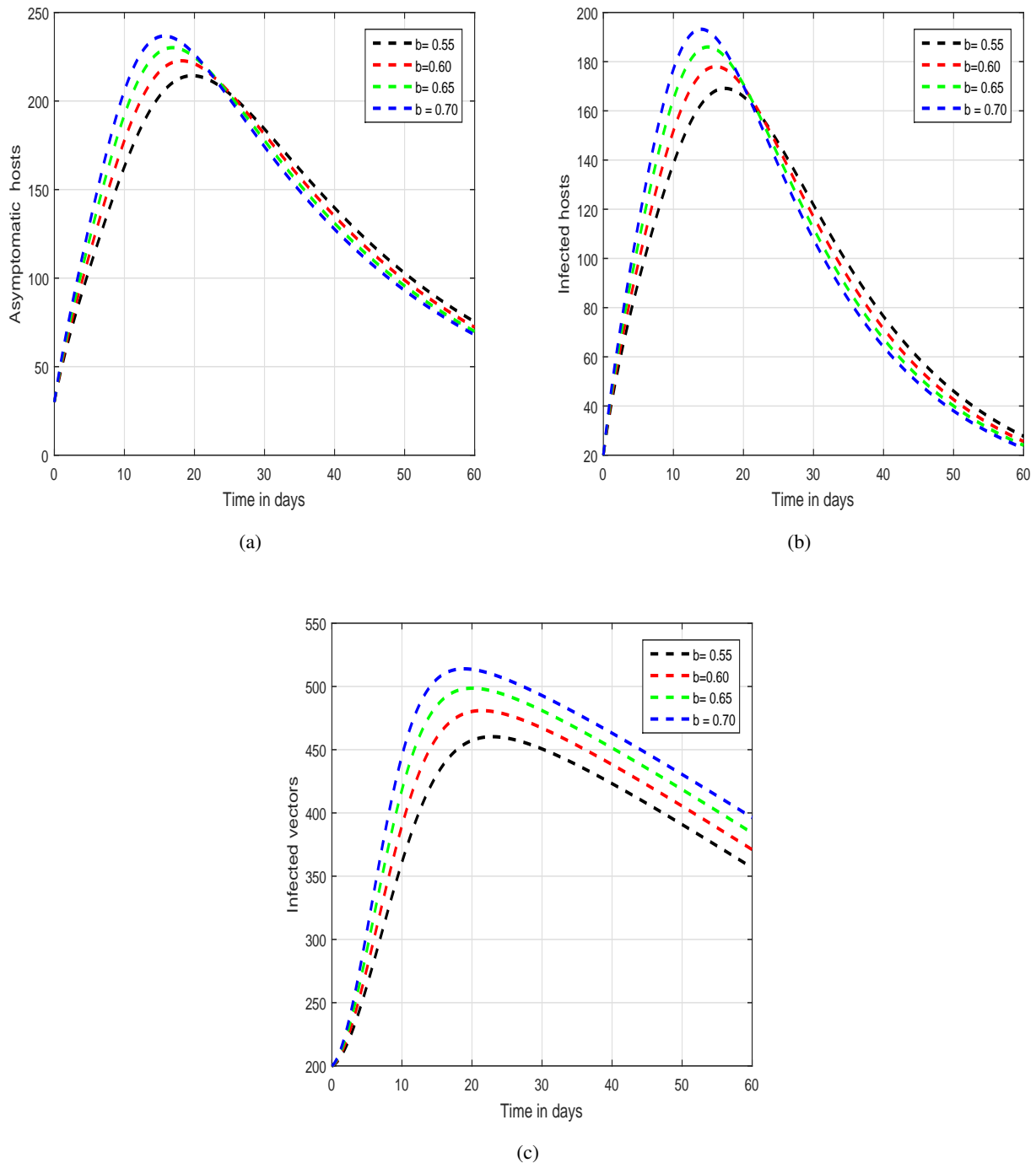


Figure 3. Depiction of the solution pathways for the recommended fractional system (3.4) for dengue infection, considering varying biting rates, i.e., b values of 0.55, 0.60, 0.65, and 0.70.

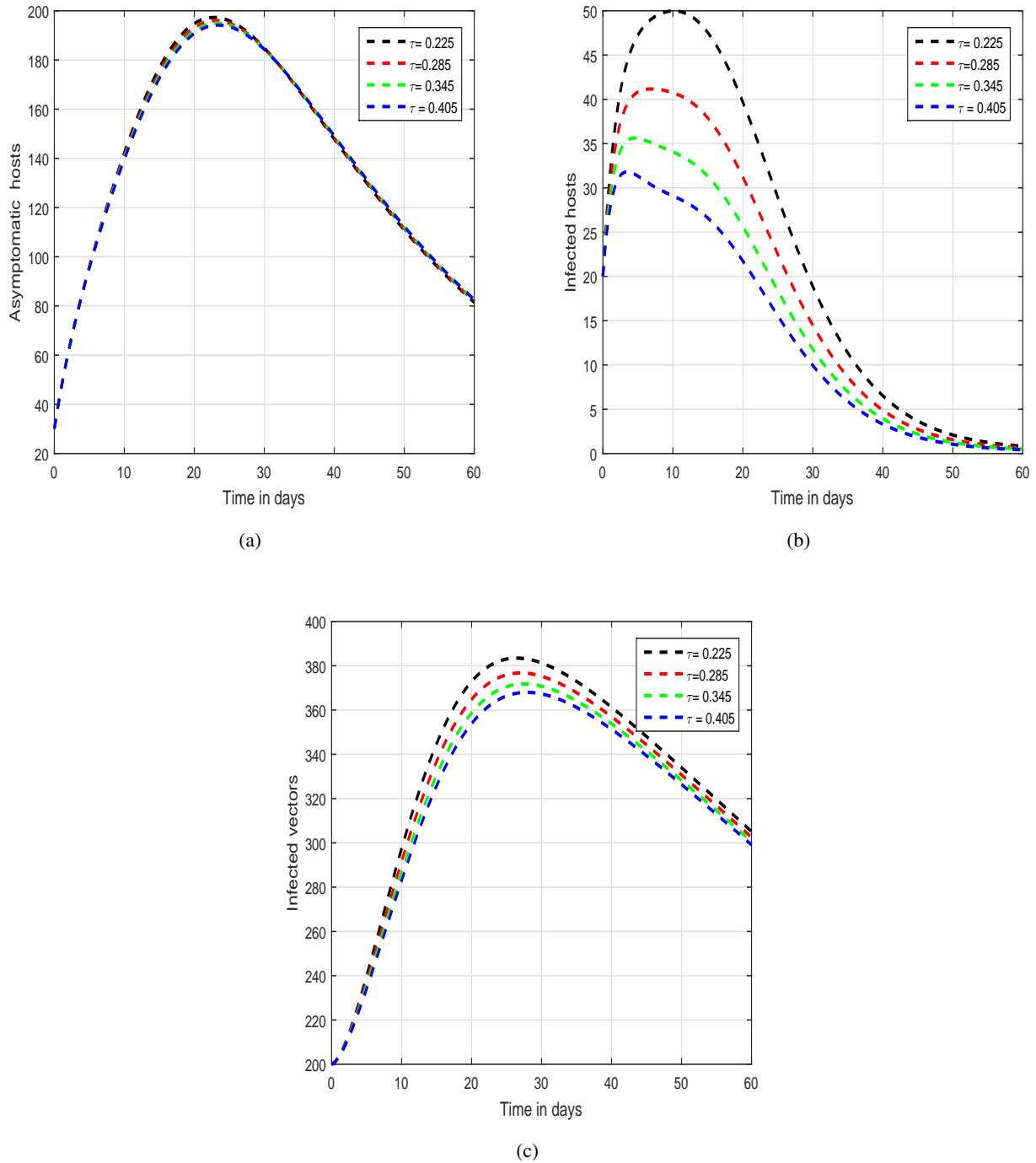


Figure 4. Temporal analysis of the impacted categories within our dengue infection model (3.4) was conducted, considering varying treatment rates denoted as τ , i.e., $\tau = 0.225, 0.285, 0.345$, and 0.405 .

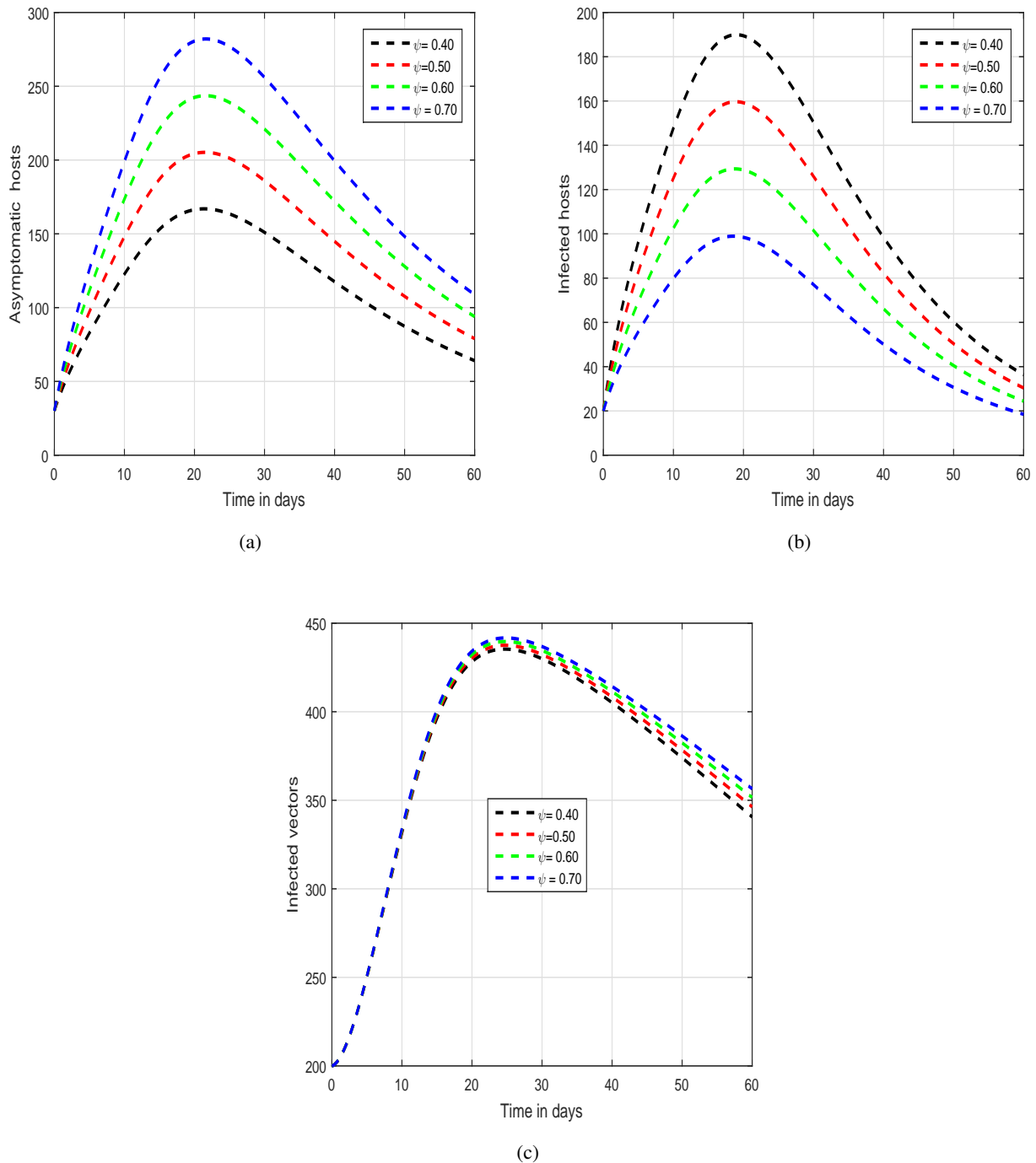


Figure 5. The infected categories of dengue infection in our model (3.4) were subjected to time series analysis while altering the carrier fraction ψ across values of $\psi = 0.40, 0.50, 0.60,$ and 0.70 .

in the most recent scenario portrayed in Figure 5, we have elucidated the variation in the prevalence of dengue infection with alterations in the carrier fraction. It is evident from the results that this factor assumes a pivotal role, possessing the potential to escalate the risk of infection within both endemic and non-endemic regions. It has been observed in these findings that the control of memory index can control the infection level of both the populations in the community. Therefore, we conclude that this parameter is attractive and should be used by the public health officials for the control of dengue.

We believe that getting vaccinated and receiving treatment are important for the control of dengue infection. In addition to this, managing the infection effectively involves using things like bed nets and insecticide sprays, along with adjusting the memory index on purpose.

7. Concluding remarks

The worldwide prevalence of dengue viral infection presents a substantial risk to public health, carrying the potential for life-threatening outcomes. At present, devising successful approaches to manage this viral malady is considered as a significant hurdle for policymakers, researchers, and public health authorities. In this work, we analyzed the dynamics of dengue infection with the effect of different control measures for public health. We presented the proposed dynamics of dengue from the perspective of a fractional framework to capture the role of memory in the transmission of dengue infection. The basic concepts and ideas of fractional theory have been introduced for the analysis of our model. It has been shown that the solutions of the model are non-negative and bounded for non-negative initial values. The existence and uniqueness of the proposed dengue model's solution were examined by using Banach's and Schaefer's frameworks, employing the fixed-point theorem. Furthermore, we have established adequate conditions for Ulam-Hyers stability of our system of dengue infection. To visualize the dynamical behavior of dengue infection, we performed different simulations with variation of the input parameters of the system. We demonstrated the pivotal roles of asymptomatic carriers, the biting rate, and the transmission probability as critical parameters that can exacerbate the difficulty of controlling dengue infection. On the other hand, the index of memory, vaccination, and treatment have the potential to effectively manage dengue infection. The results of our study emphasize the noteworthy influence of memory on the behavior of dengue, indicating its potential as a controlling factor for infection management. In our future work, we intend to explore how the dynamics of dengue infection are affected by maturation and incubation delay.

Use of AI tools declaration

The authors declare that they have not used artificial intelligence tools in the creation of this article.

Acknowledgments

Project financed by Lucian Blaga University of Sibiu through research grant LBUS-IRG-2023-09.

Conflict of interest

Hijaz Ahmad is on a special issue editorial board for AIMS Bioengineering and was not involved in the editorial review or the decision to publish this article. All authors declare that there are no competing interests. The authors declare that there is no conflict of interests regarding the publication of this paper.

References

1. Wellekens K, Betraains A, De Munter P, et al. (2022) Dengue: current state one year before WHO 2010–2020 goals. *Acta Clin Belg* 77: 436–444. <https://doi.org/10.1080/17843286.2020.1837576>
2. Basso CR, Crulhas BP, Castro GR, et al. (2021) The use of nano-enabled technologies to diagnose dengue virus infections, In: Formiga FR, Inamuddin, Severino P, *Applications of Nanobiotechnology for Neglected Tropical Diseases*, New York: Academic Press, 71–88. <https://doi.org/10.1016/B978-0-12-821100-7.00021-2>
3. World Health Organization, Dengue and Severe Dengue Fact sheets. World Health Organization, 2017. Available from: <https://www.who.int/news-room/fact-sheets/detail/dengue-and-severe-dengue>.
4. Gubler DJ (1997) Dengue and dengue hemorrhagic fever: its history and resurgence as a global public health problem, In: Gubler DJ, Kuno G, *Dengue and Dengue Hemorrhagic Fever*, London: CAB International, 1–22.
5. Guzmán MG, Kouri G, Bravo J, et al. (2002) Effect of age on outcome of secondary dengue 2 infections. *J Infect Dis* 6: 118–124. [https://doi.org/10.1016/S1201-9712\(02\)90072-X](https://doi.org/10.1016/S1201-9712(02)90072-X)
6. East S (2016) World’s first dengue fever vaccine launched in the Philippines. CNN. Available from: <https://edition.cnn.com/2016/04/06/health/dengue-fever-vaccine-philippines/index.html>.
7. Boulaaras S, Jan R, Khan A, et al. (2024) Modeling the dynamical behaviour of the interaction of T-cells and human immunodeficiency virus with saturated incidence. *Commun Theor Phys* <https://doi.org/10.1088/1572-9494/ad2368>
8. Tang TQ, Jan R, Khurshaid A, et al. (2023) Analysis of the dynamics of a vector-borne infection with the effect of imperfect vaccination from a fractional perspective. *Sci Rep-UK* 13: 14398. <https://doi.org/10.1038/s41598-023-41440-7>
9. Deebani W, Jan R, Shah Z, et al. (2023) Modeling the transmission phenomena of water-borne disease with non-singular and non-local kernel. *Comput Method Biomec* 26: 1294–1307. <https://doi.org/10.1080/10255842.2022.2114793>
10. Jan A, Srivastava HM, Khan A, et al. (2023) In vivo hiv dynamics, modeling the interaction of hiv and immune system via non-integer derivatives. *Fractal Fract* 7: 361. <https://doi.org/10.3390/fractalfract7050361>
11. Esteva L, Vargas C (1999) A model for dengue disease with variable human population. *J Math Biol* 38: 220–240. <https://doi.org/10.1007/s002850050147>
12. Tewa JJ, Dimi JL, Bowong S (2009) Lyapunov functions for a dengue disease transmission model. *Chaos Soliton Fract* 39: 936–941. <https://doi.org/10.1016/j.chaos.2007.01.069>

13. Rodrigues HS, Monteiro MTT, Torres DF (2014) Vaccination models and optimal control strategies to dengue. *Math Biosci* 247: 1–12. <https://doi.org/10.1016/j.mbs.2013.10.006>
14. Jan R, Boulaaras S (2022) Analysis of fractional-order dynamics of dengue infection with non-linear incidence functions. *T I Meas Control* 44: 2630–2641. <https://doi.org/10.1177/01423312221085049>
15. Sánchez-González G, Condé R (2023) Mathematical modeling of dengue virus serotypes propagation in Mexico. *Plos One* 18: e0288392. <https://doi.org/10.1371/journal.pone.0288392>
16. Abidemi A, Aziz NAB (2022) Analysis of deterministic models for dengue disease transmission dynamics with vaccination perspective in Johor, Malaysia. *Int J Appl Comput Math* 8: 45. <https://doi.org/10.1007/s40819-022-01250-3>
17. Phajjoo GR, Gurung DB (2015) Mathematical model of dengue fever with and without awareness in host population. *Int J Adv Eng Res Appl* 1: 239. Available from: http://www.research.net/publication/287330312_Mathematical_Model_of_Dengue_Fever_with_and_without_awareness_in_Host_Population.
18. Endy TP, Chunsuttiwat S, Nisalak A, et al. (2002) Epidemiology of inapparent and symptomatic acute dengue virus infection: a prospective study of primary school children in Kamphaeng Phet, Thailand. *Am J Epidemiol* 156: 40–51. <https://doi.org/10.1093/aje/kwf005>
19. Rowe EK, Leo YS, Wong JG, et al. (2014) Challenges in dengue fever in the elderly: atypical presentation and risk of severe dengue and hospita-acquired infection. *Plos Neglect Trop D* 8: e2777. <https://doi.org/10.1371/journal.pntd.0002777>
20. Rehman ZU, Boulaaras S, Jan R, et al. (2024) Computational analysis of financial system through non-integer derivative. *J Comput Sci* 75: 102204. <https://doi.org/10.1016/j.jocs.2023.102204>
21. Ahmad I, Ali I, Jan R, et al. (2023) Solutions of a three-dimensional multi-term fractional anomalous solute transport model for contamination in groundwater. *Plos one* 18: e0294348. <https://doi.org/10.1371/journal.pone.0294348>
22. Thounthong P, Khan MN, Hussain I, et al. (2018) Symmetric radial basis function method for simulation of elliptic partial differential equations. *Mathematics* 6: 327. <https://doi.org/10.3390/math6120327>
23. Ahmad I, Ahsan M, Hussain I, et al. (2019) Numerical simulation of PDEs by local meshless differential quadrature collocation method. *Symmetry* 11: 394. <https://doi.org/10.3390/sym11030394>
24. Ahmad I, Ahsan M, Din Z, et al. (2019) An efficient local formulation for time-dependent PDEs. *Mathematics* 7: 216. <https://doi.org/10.3390/math7030216>
25. Wang F, Ahmad I, Ahmad H, et al. (2021) Meshless method based on RBFs for solving three-dimensional multi-term time fractional PDEs arising in engineering phenomenons. *J King Saud Univ Sci* 33: 101604. <https://doi.org/10.1016/j.jksus.2021.101604>
26. Li JF, Ahmad I, Ahmad H, et al. (2020) Numerical solution of two-term time-fractional PDE models arising in mathematical physics using local meshless method. *Open Phy* 18: 1063–1072. <https://doi.org/10.1515/phys-2020-0222>

27. Shakeel M, Khan MN, Ahmad I, et al. (2023) Local meshless collocation scheme for numerical simulation of space fractional PDE. *Thermal Sci* 27: 101–109. <https://doi.org/10.2298/TSCI23S1101S>
28. Ahmad I, Bakar AA, Ali I, et al. (2023) Computational analysis of time-fractional models in energy infrastructure applications. *Alex Eng J* 82: 426–436. <https://doi.org/10.1016/j.aej.2023.09.057>
29. Arnous AH, Hashemi MS, Nisar KS, et al. (2024) Investigating solitary wave solutions with enhanced algebraic method for new extended Sakovich equations in fluid dynamics. *Results Phys* 57: 107369. <https://doi.org/10.1016/j.rinp.2024.107369>
30. Ain QT, Khan A, Abdeljawad T, et al. (2023) Dynamical study of varicella-zoster virus model in sense of mittag-leffler kernel. *Int J Biomath* 17: 2350027. <https://doi.org/10.1142/S1793524523500274>
31. Mohammed PO, Sarikaya MZ (2020) On generalized fractional integral inequalities for twice differentiable convex functions. *J Comput Appl Math* 372: 112740. <https://doi.org/10.1016/j.cam.2020.112740>
32. tul Ain Q, Khan A, Ullah MI, et al. (2022) On fractional impulsive system for methanol detoxification in human body. *Chaos Soliton Fract* 160: 112235. <https://doi.org/10.1016/j.chaos.2022.112235>
33. Mohammed PO, Srivastava HM, Baleanu D, et al. (2022) Monotonicity results for nabla riemann–liouville fractional differences. *Mathematics-basel* 10: 2433. <https://doi.org/10.3390/math10142433>
34. Lin Z, Wang H (2021) Modeling and application of fractional-order economic growth model with time delay. *Fractal Fract* 5: 74. <https://doi.org/10.3390/fractalfract5030074>
35. Liu X, Ahsan M, Ahmad M, et al. (2021) Applications of haar wavelet-finite difference hybrid method and its convergence for hyperbolic nonlinear Schrödinger equation with energy and mass conversion. *Energies* 14: 7831. <https://doi.org/10.3390/en14237831>
36. Wang F, Hou E, Ahmad I, et al. (2021) An efficient meshless method for hyperbolic telegraph equations in (1 + 1) dimensions, *CMEC-Comput Model Eng* 128: 687–698. <https://doi.org/10.32604/cmec.2021.014739>
37. He JH, Ain QT (2020) New promises and future challenges of fractal calculus: from two-scale thermodynamics to fractal variational principle. *Therm Sci* 24: 659–681. <https://doi.org/10.2298/TSCI200127065H>
38. Tul Ain Q, Sathiyaraj T, Karim S, et al. (2022) Abc fractional derivative for the alcohol drinking model using two-scale fractal dimension. *Complexity* 2022. <https://doi.org/10.1155/2022/8531858>
39. Chaves LF, Harrington LC, Keogh CL, et al. (2010) Blood feeding patterns of mosquitoes: random or structured. *Front Zool* 7: 1–11. <https://doi.org/10.1186/1742-9994-7-3>
40. Vinauger C, Buratti L, Lazzari CR (2011) Learning the way to blood: first evidence of dual olfactory conditioning in a blood-sucking insect, *Rhodnius prolixus*. i. appetitive learning. *J Exp Biol* 214: 3032–3038. <https://doi.org/10.1242/jeb.056697>
41. Mohammeda PO, Fernandezb A (2023) Integral inequalities in fractional calculus with general analytic kernels. *Filomat* 37: 3659–3669. <https://doi.org/10.2298/FIL2311659M>

42. Kilbas A, Srivastava HM, Trujillo JJ, et al. (2006) *Theory and Applications of Fractional Differential Equations*. Netherlands: Elsevier.
43. Anjum N, He CH, He JH (2021) Two-scale fractal theory for the population dynamics. *Fractals* 29: 2150182. <https://doi.org/10.1142/S0218348X21501826>
44. Wang KL, He CH (2019) A remark on wang's fractal variational principle. *Fractals* 27: 1950134. <https://doi.org/10.1142/S0218348X19501342>
45. Belay MA, Abonyo OJ, Theuri DM, et al. (2023) Mathematical model of hepatitis B disease with optimal control and cost-effectiveness analysis. *Comput Math Method M* 2023: 1–29. <https://doi.org/10.1155/2023/5215494>
46. Kinfe H, Sendo EG, Gebremedhin KB (2021) Prevalence of hepatitis B virus infection and factors associated with hepatitis B virus infection among pregnant women presented to antenatal care clinics at adigrat general hospital in northern Ethiopia. *Int J Womens Health* 13: 119–127. <https://doi.org/10.2147/IJWH.S280806>
47. Ding Y, Ye H (2009) A fractional-order differential equation model of HIV infection of CD4⁺ T-cells. *Math Comput Model* 50: 386–392. <https://doi.org/10.1016/j.mcm.2009.04.019>
48. Hincal E, Alsaadi SH (2021) Stability analysis of fractional order model on corona transmission dynamics. *Chaos Soliton Fract* 143: 110628. <https://doi.org/10.1016/j.chaos.2020.110628>
49. Ullam S (1940) Some questions in analysis, In: Ullam S, *Problems in Modern Mathematics*, New York: Wiley, 63–82.
50. Hyers DH (1941) On the stability of the linear functional equation. *P Natl A Sci* 27: 222–224. <https://doi.org/10.1073/pnas.27.4.222>
51. Rassias TM (1978) On the stability of the linear mapping in banach spaces. *P Am Math Soc* 72: 297–300. <https://doi.org/10.1073/pnas.27.4.222>
52. Benkerrouche A, Souid MS, Etemad S, et al. (2021) Qualitative study on solutions of a Hadamard variable order boundary problem via the Ulam–Hyers–Rassias stability. *Fractal fract* 5: 108. <https://doi.org/10.3390/fractalfract5030108>



AIMS Press

© 2024 the Author(s), licensee AIMS Press. This is an open access article distributed under the terms of the Creative Commons Attribution License (<https://creativecommons.org/licenses/by/4.0>)